Preprint

Tunability of Recording Head Protrusion by Use of Embedded Dual Heaters

Qilong Cheng, David B. Bogy

DOI: https://doi.org/10.1007/s11249-022-01606-2

To appear in: *Tribology Letters*

Received date: 08 March 2022

Accepted date: 25 April 2022

Please cite this article as: Cheng, Q., Bogy, D.B. Tunability of Recording Head Protrusion by Use of Embedded Dual Heaters. Tribol Lett 70, 64 (2022). https://doi.org/10.1007/s11249-022-01606-2

Tunability of recording head protrusion by use of embedded dual heaters

Qilong Cheng[1*] and David B. Bogy[1]

[1*]University of California at Berkeley, Berkeley, CA 94720, USA.

*Corresponding author(s). E-mail(s): qlcheng@berkeley.edu;

Abstract

In hard disk drives (HDDs), a recording head and a recording disk constitute a high-speed sliding system: head-disk interface, where the head with a prescribed thermal protrusion on its surface flies over the rotating disk at an air gap $<$ 1–2 nm. Currently, the magnetic recording operations involve two embedded joule heaters in the recording head to generate two thermal protrusions and thus improve the device performance in data writing and data reading. In this study, we performed touchdown experiments to induce frictional interaction between the head and the disk and characterize the total head protrusion due to the dual heaters. The experimental results demonstrate that the head protrusion can be tuned by use of the dual heaters, and that the touchdown area can be controlled precisely.

Keywords: thermal protrusion; dual heaters; head-disk interface; magnetic recording

1 Introduction

Data are indispensable and play an essential role in people's lives. According to the International Data Corporation, the data generated worldwide are growing explosively and are expected to grow more rapidly in the future [1]. To store the enormous amount of data, hard disk drives (HDDs) are still the major data storage medium in data centers due to their low cost and longevity as compared to solid state drives (SSDs) [2]. Conventional HDD technology utilizes a recording head to perform data writing and data reading and a recording disk to store the data. The head and the disk constitute a high-speed sliding system: head-disk interface, where the spacing between the head and the disk has decreased from micrometers to nanometers [3, 4]. Nowadays, the initial head-disk spacing is $\sim$ 10–15 nm which is controlled by the air bearing design. The spacing is further reduced by energizing a joule heater that is embedded in the head [5]. The heater generates a microscale protrusion on the head surface by thermal expansion to achieve an air gap $<$ 1–2 nm between the protrusion surface and the disk surface, which is called the fly height. Therefore, the heater is also known as the thermal fly-height control (TFC). With such a small physical spacing, data reading/writing can be performed using the read/write transducers (reader/writer) in the head.

Currently, the magnetic recording operations involve two embedded joule heaters in the head to realize different and independent fly heights at the read and write transducers, respectively [6, 7]. By use of the dual heaters, a larger fly height reduction at the transducers can be achieved, and the heater actuation efficiency (ratio of fly height reduction to the maximum thermal protrusion) can be improved [8–11]. Past research on this topic mainly focuses on modelling and numerical simulations [12, 13], or dual thermal protrusions of one laser-induced protrusion and one joule heater protrusion [14]. Few experimental papers on the dual joule heaters have hitherto been published. In this study, by inducing frictional interaction between the head and the disk, touchdown experiments were performed to evaluate the thermal protrusions of the dual heaters. It is demonstrated that the head protrusion can be tuned by use of the dual heaters, and that the touchdown area can be controlled precisely.

2 Experimental setup

Figure 1(a) shows a schematic diagram of the head-disk interface, where the dual heaters are highlighted. Heater-1 is the commonly used heater that is embedded near the reader, while heater-2 is located near the writer. They can generate two thermal protrusions as the black dashed lines drawn in Figure 1(a). The red dashed line is the sum of the two protrusion profiles, and it corresponds to the actual total protrusion. The head is also integrated with a nanoscale thermistor near its surface (Figure 1(c)), which is typically used to detect the head-disk contact events or measure the head temperature [15–20]. When the heaters are energized, their protrusions form due to thermal expansion, which brings the thermistor near the surface of the total protrusion as the arrow shown in Figure 1(a). By tuning the dual heaters' powers, the total protrusion can be adjusted, and the thermistor can be at the peak of the total protrusion when using proper powers for the dual heaters.

The head-disk interface touchdown refers to the case where the thermal protrusion is large enough to cover the head-disk spacing and hence induce mechanical contact between the head and the rotating disk. The component-level experimental setup of touchdown is shown in Figure 1(b). The head flies over the rotating disk with the components (the heaters and the thermistor) controlled by a PC via a data acquisition (DAQ) toolbox. To perform the

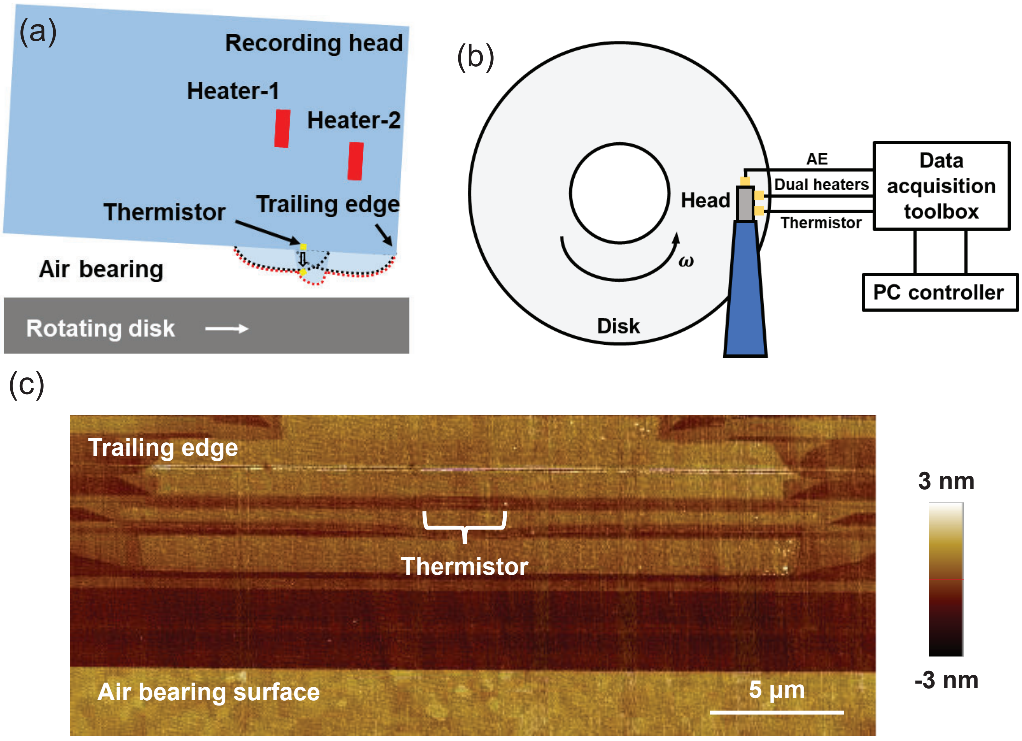

Fig. 1 (a) A schematic diagram (not to scale) of the head-disk interface showing the dual heaters and their protrusions (black dashed line: respective protrusion profiles; red dashed line: total protrusion profile). (b) A schematic diagram of the experimental setup. (c) An atomic force microscopy (AFM) image of the head surface showing the thermistor.

touchdowns, one heater was biased at a prescribed constant power, and the other heater was energized with an increasing power in steps such that the head-disk spacing was gradually reduced to zero. The touchdowns, namely the contact between the head and the disk, were indicated by an acoustic emission (AE) sensor that was attached to the head fixture [21].

3 Results and Discussion

Figure 2 shows the temperature rise measured by the thermistor and the AE root mean square (RMS) signal during the touchdowns with an increasing heater-1 power P_1 and a constant heater-2 power P_2. Figure 2(a) shows that the thermistor undergoes a temperature translation ~ 97.8 °C when the heater-1 is OFF and the heater-2 power increases by 100.0 mW (heater-2 heating rate 0.98 °C/mW at the thermistor). Then, with the increasing power of heater-1, the head-disk spacing is reduced and contact occurs, which can be observed from the thermistor's cooling in Figure 2(a) and the AE RMS signal's ramp-up in Figure 2(b). At a larger prescribed heater-2 power, a thermal protrusion by heater-2 exists in the head-disk interface, and thus a smaller heater-1 power is needed to realize contact. For example, Figure 2(b) shows that the initial touchdown power (TDP, defined as the heater power at the contact onset) is 128.2 mW using the heater-1 alone, while the TDP by heater-1 becomes 23.0 mW with a prescribed heater-2 power of 100.0 mW. The experiments were

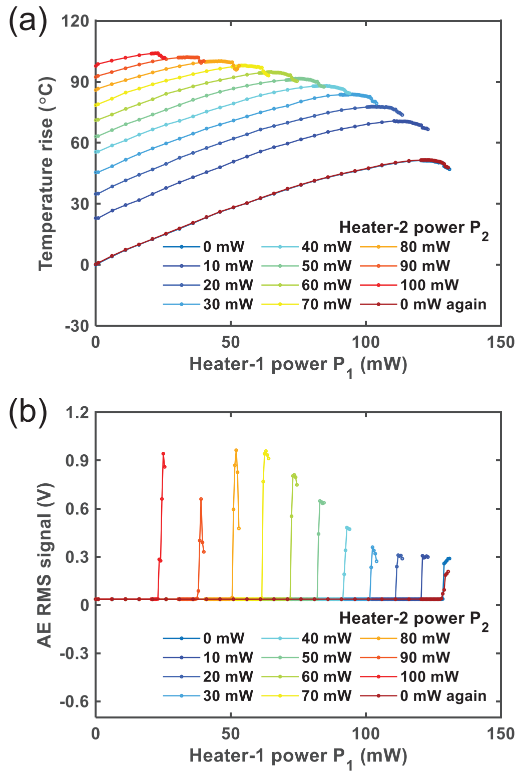

Fig. 2 (a) The temperature rise and (b) the AE RMS signal as a function of the heater-1 power P_1 during the touchdowns with a constant prescribed heater-2 power P_2.

performed in the sequence of the legends in Figure 2. Finally, the 0 mW curve was repeated, and it coincides with the first 0 mW curve, which confirms that the head-disk interface does not change after multiple touchdowns.

To investigate the nanoscale heat transfer across the interface, the rate of change of the thermistor temperature rise with the heater-1 power, dT/dP_1, is extracted from Figure 2(a) and plotted in Figure 3, where the heater-1 power is denoted as the power relative to the contact onset with zero being the contact onset indicated by AE. The relative heater power essentially describes the spacing between the head protrusion and the disk surface. Figure 3 shows that the dT/dP_1 monotonically decreases with the spacing and increases after contact occurs, which features a minimum near 1 mW. The dT/dP_1 indicates the heat transfer across the head-disk interface. When the spacing decreases to zero, the stronger heat transfer carries the heater's joule heating away and cools the thermistor, resulting in a smaller dT/dP_1. After contact occurs, the minimum $(dT/dP_1)_{\min}$ corresponds to the maximum of total heat transfer including air conduction, phonon heat conduction, contact heat conduction and frictional heating [22–24]. Later, with the heater-1 power exceeding the TDP, the frictional heating dominates due to the increasing normal force, and the dT/dP_1 accordingly rises. Therefore, if the thermistor is at the peak of the total head protrusion and touches the moving disk surface first, the thermistor should have a smallest $(dT/dP_1)_{\min}$ due to the strongest heat transfer.

Figure 4 plots the $(dT/dP_1)_{\min}$ from Figure 3 as a function of the prescribed heater-2 power P_2. The curve has the smallest $(dT/dP_1)_{\min}$ when the heater-2

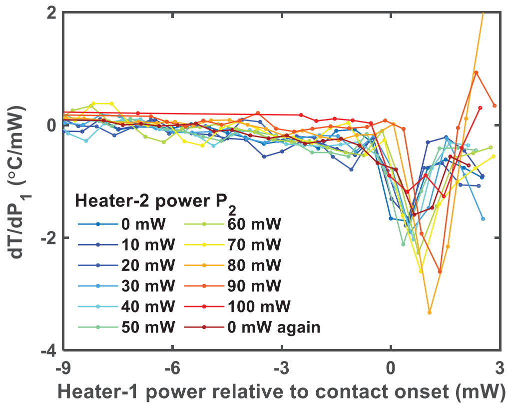

Fig. 3 The dT/dP_1 as a function of the heater-1 power (relative to contact onset) during the touchdowns with a constant prescribed heater-2 power P_2.

power P_2 is 80.0 mW, indicating that the thermistor comes into contact with the disk surface first at this condition, where the heater-1 power P_1 is 51.0 mW. To put this in another way, the thermistor is located at the peak of the total protrusion with the heater-1 power P_1 of 51.0 mW and the heater-2 power P_2 of 80.0 mW. Therefore, by arranging the dual heaters' powers, the total protrusion's shape can be changed, and the touchdown area can be controlled at the thermistor's location.

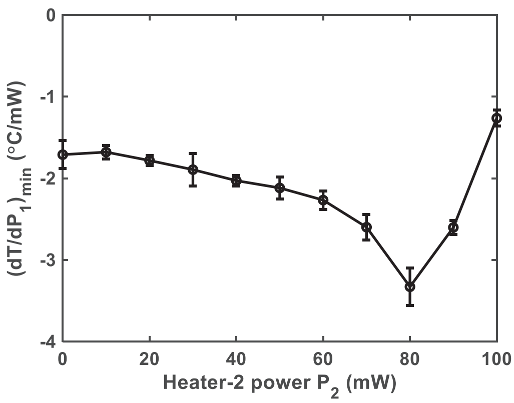

Fig. 4 The minimum of the dT/dP_1 as a function of the heater-2 power P_2 during the touchdowns achieved by increasing the heater-1 power.

Figure 5 shows the experiments performed in the opposite way, where the heater-1 was biased with a constant power P_1 and the heater-2 had an increasing power P_2. Figure 5(a-b) show the temperature rise and the AE RMS signal during the touchdowns achieved by increasing the heater-2 power P_2. The thermistor's temperature translation by the heater-1 is 0.48 °C/mW, which is much smaller than that by heater-2 (0.98 °C/mW) as shown in Figure 2. The heating rate is dependent on the heater's parameters (size, distance from the thermistor) and the material parameters near the thermistor (thermal conductivity). For example, the thermistor is surrounded by metal shields (Ni, Fe, and Cu) as shown in Figure 1(c), which could affect the temperature at the thermistor location because the metals usually have higher thermal conductivity

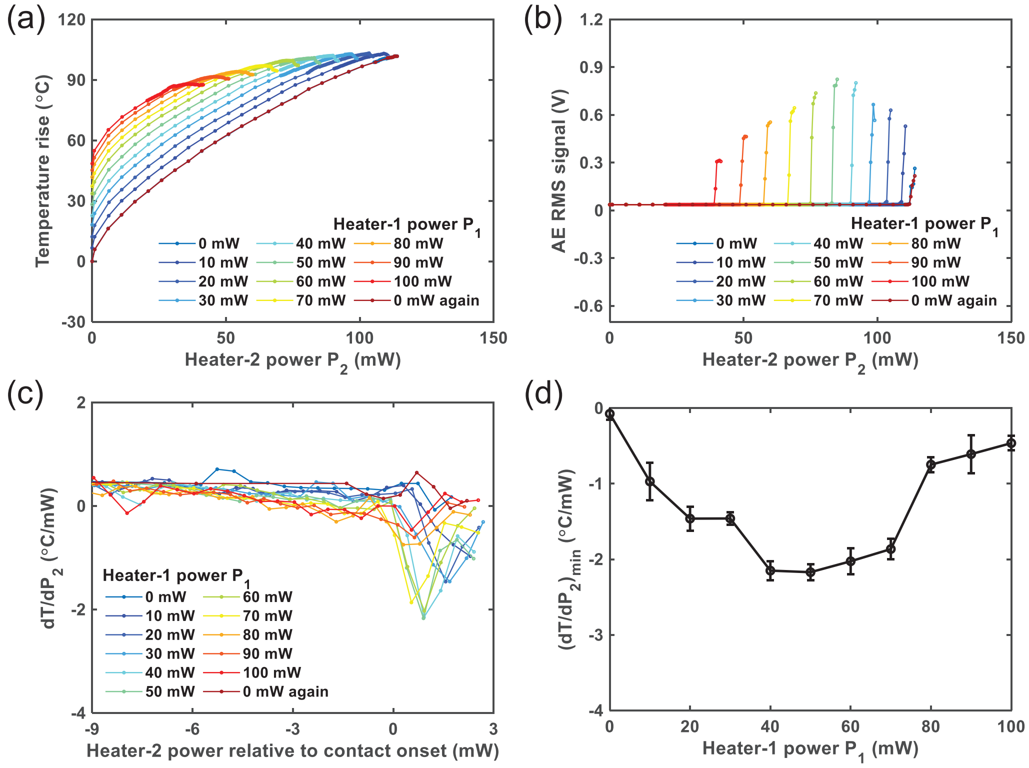

Fig. 5 (a) The temperature rise and (b) the AE RMS signal as a function of the heater-2 power P_2 during the touchdown with a constant prescribed heater-1 power P_1. (c) The dT/dP_2 as a function of the heater-2 power (relative to contact onset) during the touchdown with a constant prescribed heater-1 power P_1. (d) The minimum of the dT/dP_2 as a function of the heater-1 power P_1 during the touchdowns achieved by increasing heater-2 power.

than the underlying alumina slider body (1.8 W/(m·K) [8]). Figure 5(c-d) show the extracted dT/dP_2 and $(dT/dP_2)_{\min}$ during the touchdown process. Similarly, the thermistor dT/dP_2 has a minimum near 1 mW after contact occurs. Figure 5(d) shows that the $(dT/dP_2)_{\min}$ is close to zero when the heater-1 power P_1 is 0 mW, indicating that the thermistor has almost no cooling during the touchdown, which can also be seen in Figure 5(a). The reason is that the thermistor is relatively far away from the center of the heater-2 protrusion (Figure 1(a)), and thus it can not sense any cooling when the heater-2 protrusion alone touches the disk surface. The smallest $(dT/dP_2)_{\min}$ in Figure 5(d) occurs at the heater-1 power P_1 of 50.0 mW, where the heater-2 power P_2 is 83.5 mW from Figure 5(b-c). The results illustrate that the thermistor is at the peak of the total protrusion with the heater-1 power of P_1 50.0 mW and the heater-2 power P_2 of 83.5 mW. The needed heater-2 power is larger than that for the heater-1, which confirms the thermistor's larger distance from the center of the heater-2 protrusion. Also, compared to the obvious smallest $(dT/dP_1)_{\min}$ in Figure 4 (-3.3 °C/mW), the observed poor sensitivity of the smallest $(dT/dP_2)_{\min}$ in Figure 5(d) (-2.2 °C/mW) further validates that the thermistor is positioned farther from the heater-2's projection on the head surface, namely its protrusion center, as the same power change dP at the heater-1 can induce a larger temperature drop at the thermistor. The dual heaters' powers measured here are 50.0 mW and 83.5 mW, which is very close to the circumstance derived from Figure 2–Figure 4 (51.0 mW and 80.0 mW). If heater efficiencies (ratio of protrusion size to applied power, from ~ 0.14 nm/mW at the initial spacing to ~ 0.03 nm/mW near touchdown [25]) are assumed to be only dependent on the head-disk spacing, the thermistor remains at the peak of the total head protrusion when the heater-1/heater-2 powers have a ratio of 0.62.

4 Conclusion

In conclusion, we performed the touchdown experiments to investigate the dual thermal protrusions. The head temperature was measured during the touchdowns by use of the dual heaters. One heater was biased at a prescribed constant power, and the other heater was energized with an increasing power to realize touchdowns, or vice versa. Both the schemes show that the thermistor undergoes the strongest heat transfer (smallest $(dT/dP)_{\min}$) when contact occurs under the circumstance of the heater-1 power ~ 50 mW and the heater-2 power ~ 80 mW. And to sense the maximum heat transfer, the thermistor needs to be at the peak of the overall protrusion of the dual heaters such that it can touch the moving disk surface first. Therefore, it is demonstrated that the head protrusion can be tuned by use of the dual heaters, and that the touchdown area can be controlled precisely. Moreover, the head protrusion can be used as a mechanical approach to address the laser-induced material accumulation (smear) issue in heat-assisted magnetic recording (HAMR) [26]. This study contributes to the protrusion management in the head-disk interface, and hence is expected to be useful for the HAMR smear management too.

Acknowledgments. The work was supported by Computer Mechanics Laboratory at Department of Mechanical Engineering, UC Berkeley. We thank Robert Smith, Erhard Schreck, Qing Dai, Sukumar Rajauria and Tan Trinh of Western Digital for supplying the components and providing insightful discussions.

Declarations

Conflict of interest. The authors declare that they have no conflict of interest.

References

[1] Reinsel, D., Gantz, J., Rydning, J.: The digitization of the world from edge to core. Framingham: International Data Corporation, 16 (2018)

[2] Fontana, R., Decad, G.: The 2018 storage landscape-an 11 year perspective (2008-2019): Lto tape media hdd nand. In: the 2018 Storage Landscape–Library of Congress (2019)

[3] Zhu, L.-Y., Bogy, D.: A comparison of head-to-disk spacing fluctuation on hard and stretch-surface recording disks. IEEE Transactions on Magnetics **23**(5), 3447–3449 (1987)

[4] Grochowski, E., Hoyt, R.F.: Future trends in hard disk drives. IEEE Transactions on Magnetics **32**(3), 1850–1854 (1996)

[5] Meyer, D.W., Kupinski, P.E., Liu, J.C.: Slider with temperature responsive transducer positioning. Google Patents. US Patent 5,991,113 (1999)

[6] Hsiao, W.-C.D., Shen, X.: Magnetic head with self compensating dual thermal fly height control. Google Patents. US Patent 8,634,167 (2014)

[7] Contreras, J., McFadyen, I.R., Schreck, E.: Implementing dual partially independent thermal flyheight control (TFC) for hard disk drives. Google Patents. US Patent 9,564,163 (2017)

[8] Kurita, M., Xu, J., Tokuyama, M., Nakamoto, K., Saegusa, S., Maruyama, Y.: Flying-height reduction of magnetic-head slider due to thermal protrusion. IEEE Transactions on Magnetics **41**(10), 3007–3009 (2005)

[9] Suk, M., Miyake, K., Kurita, M., Tanaka, H., Saegusa, S., Robertson, N.: Verification of thermally induced nanometer actuation of magnetic recording transducer to overcome mechanical and magnetic spacing challenges. IEEE Transactions on Magnetics **41**(11), 4350–4352 (2005)

[10] Juang, J.-Y., Bogy, D.B.: Air-bearing effects on actuated thermal poletip protrusion for hard disk drives. Journal of Tribology **129**(3), 570–578 (2007)

[11] Li, H., Yin, C.-T., Talke, F.E.: Thermal insulator design for optimizing the efficiency of thermal flying height control sliders. Journal of Applied Physics **105**(7), 07–122 (2009)

[12] Zheng, H., Li, H., Talke, F.E.: Numerical simulation of a thermal flying height control slider with dual heater and insulator elements. IEEE Transactions on Magnetics **45**(10), 3628–3631 (2009)

[13] Zheng, H., Li, H., Amemiya, K., Talke, F.E.: The effect of write current on thermal flying height control sliders with dual heater/insulator elements. Microsystem Technologies **17**(5-7), 959–964 (2011)

[14] Shaomin, X., Bogy, D.B.: Flying height modulation for a dual thermal protrusion slider in heat assisted magnetic recording (hamr). IEEE transactions on magnetics **49**(10), 5222–5226 (2013)

[15] Xu, J., Shimizu, Y., Furukawa, M., Li, J., Sano, Y., Shiramatsu, T., Aoki,

Y., Matsumoto, H., Kuroki, K., Kohira, H.: Contact/clearance sensor for hdi subnanometer regime. IEEE transactions on magnetics **50**(3), 114–118 (2014)

[16] Wu, H., Xiong, S., Canchi, S., Schreck, E., Bogy, D.: Nanoscale heat transfer in the head-disk interface for heat assisted magnetic recording. Applied Physics Letters **108**(9), 093106 (2016)

[17] Ma, Y., Ghafari, A., Budaev, B., Bogy, D.: Controlled heat flux measurement across a closing nanoscale gap and its comparison to theory. Applied Physics Letters **108**(21), 213105 (2016)

[18] Ma, Y., Ghafari, A., Budaev, B.V., Bogy, D.B.: Measurement and simulation of nanoscale gap heat transfer using a read/write head with a contact sensor. IEEE Transactions on Magnetics **53**(2), 1–5 (2016)

[19] Cheng, Q., Sakhalkar, S., Ghafari, A., Ma, Y., Bogy, D.: Dependence of nanoscale heat transfer across a closing gap on the substrate material and ambient humidity. Applied Physics Letters **116**(21), 213102 (2020)

[20] Cheng, Q., Rajauria, S., Schreck, E., Smith, R., Wang, N., Reiner, J., Dai, Q., Bogy, D.: Precise nanoscale temperature mapping in operational microelectronic devices by use of a phase change material. Scientific reports **10**(1), 1–8 (2020)

[21] Rajauria, S., Ruiz, O., Canchi, S.V., Schreck, E., Dai, Q.: Electrostatically tunable adhesion in a high speed sliding interface. Physical Review Letters **120**(2), 026101 (2018)

[22] Zhang, S., Bogy, D.: A heat transfer model for thermal fluctuations in a thin slider/disk air bearing. International journal of heat and mass transfer **42**(10), 1791–1800 (1999)

[23] Chen, D., Liu, N., Bogy, D.B.: A phenomenological heat transfer model for the molecular gas lubrication system in hard disk drives. Journal of Applied Physics **105**(8), 084303 (2009)

[24] Sakhalkar, S., Cheng, Q., Ghafari, A., Bogy, D.: Investigation of heat transfer across a nanoscale air gap between a flying head and a rotating disk. Journal of Applied Physics **128**(8), 084301 (2020)

[25] Cheng, Q., Wang, H., Sakhalkar, S.V., Bogy, D.B.: Measurement of angstrom-level laser induced protrusion using touchdown in heat-assisted magnetic recording. Applied Physics Letters **117**(15), 153105 (2020)

[26] Cheng, Q., Bogy, D.B.: Experimental study of smear formation and removal in heat-assisted magnetic recording. Tribology International **165**,

107258 (2022)